Lab on a Chip

Accepted Manuscript

ROYAL SOCIETY OF CHEMISTRY

www.rsc.org/loc

Lab on a Chip

RSCPublishing

ARTICLE

Transportation, Dispersion and Ordering of Dense Colloidal Assemblies by Magnetic Interfacial Rotaphoresis

Cite this: DOI: 10.1039/xoxxoooooox

Received ooth January 2012,
Accepted ooth January 2012

DOI: 10.1039/xoxxoooooox

www.rsc.org/

A. van Reenen,[a] A. M. de Jong[a] and M. W. J. Prins[a,b],

Colloidal systems exhibit intriguing assembly phenomena with impact in a wide variety of technological fields. The use of magnetically responsive colloids allows one to exploit interactions with an anisotropic dipolar nature. Here, we reveal magnetic interfacial rotaphoresis – a magnetically-induced rotational excitation that imposes a translational motion to colloids by strong interaction with a solid-liquid interface – as a means to transport, disperse, and order dense colloidal assemblies. By balancing magnetic dipolar and hydrodynamic interactions at a symmetry-breaking interface, rotaphoresis effectuates a translational dispersive motion of the colloids and surprisingly transforms large and dense multilayer assemblies into single-particle layers with quasi-hexagonal ordering, within seconds and with velocities of mm/s. We demonstrate the application of interfacial rotaphoresis to enhance molecular target capture, showing an increase of the molecular capture rate by more than an order of magnitude.

1 Introduction

Colloidal assembly processes are widely studied because the resulting ordered particle structures display unique properties and create functionalities in fields such as photonics[1,2], electronics[3], sensing[4,5], and materials synthesis[2,6]. Magnetic interactions have been employed to assemble magnetic particles[7–9] into a variety of configurations such as chains[10–17], planar structures[15,18–24] and three-dimensional superstructures[9,19]. The assemblies have been studied in the context of photonic crystals[15], fluid flow generation[10–12,25], biosensing[13,21,26,27], artificial membranes[20] and surface friction gradients[28]. In magnetic assembly processes, the particles arrange themselves dominantly by dipolar magnetic interactions[7]. The dipolar potential energy is minimized by aligning the dipoles, and since dipolar forces scale as the inverse fourth power of the distance between the dipoles, magnetically driven assembly processes generally lead to chains and packed clusters of particles, which limits the versatility and applicability of magnetic colloids [26,27,29,30].

To prevent alignment, the energy minimum of the aligned configuration should become inaccessible, which requires forces other than only magnetic dipolar forces in the assembly process. Studies with ferromagnetic objects, captured in a fluid-fluid interface by surface tension and then exposed to time-dependent magnetic fields, have shown that hydrodynamic interactions are able to perturb the magnetic alignment process[31–33]. Hydrodynamic interactions can also perturb the alignment process of magnetic particles in bulk fluid. Studies on magnetic colloids exposed to rotating magnetic fields in bulk fluid revealed the formation of particle chains with cyclical breaking-and-reformation behavior[11,34]. Due to hydrodynamic interactions the chains are periodically broken, but they repeatedly regain their aligned state, so overall the chain structures remain present in the fluid. In a recent study we have shown that it is possible to break up chains of magnetic particles near a solid-liquid interface, by applying a magnetic field perpendicular to the interface in the presence of a field gradient[35]. This perpendicular-field method breaks particle chains, but it does not achieve complete disaggregation, and the method is only effective in the limit of low particle densities. Yet the ability to manipulate high densities and high numbers of colloids is very important for colloid-based functional materials and devices[6, 28]. To our knowledge, there is not yet a method available to robustly transport, disperse and order dense colloidal assemblies on a surface.

Here we report a study of colloidal assembly processes in a new configuration, namely *rotating magnetic fields operating on dense colloidal assemblies under the condition of strong interfacial interaction*. To our surprise, the experiments have revealed a variety of well-controlled assembly phenomena that are generically applicable: rapid transportation, complete dispersion, and sub-monolayer ordering. We refer to the assembly phenomena briefly as 'magnetic interfacial rotaphoresis', since magnetically-induced rotation generates

translation and spreading of particles over an interface. The phenomena appear over a wide range of colloid densities: from massive disordered multilayer assemblies down to dilute ordered single-particle layers; and the phenomena are seen for a wide range of biochemical conditions and colloid sizes (500 nm – 2.8 μm in our experiments).

2 Methods

Magnetic interfacial rotaphoresis was studied in experiments using ∅2.8 μm-sized superparamagnetic particles (M270, Dynal Biotech), suspended in undiluted phosphate buffered saline containing 0.1 m% bovine serum albumin (BSA; Merck) and 0.02% Tween-20 (Thermo Scientific). Experiments with other particle types and sizes (500 nm –2.8 μm) are described in the Supplementary Methods A and B. Particle suspensions (diluted to ~0.5 mg/mL) were pipetted into 38 μL fluid chambers (Hybridization chambers, ∅9 mm, height = 0.6 mm; Electron Microscopy Sciences) with a glass bottom surface, blocked with BSA before use. The particles were imaged with a high speed camera (Redlake MotionPro X3) that was mounted on a Leica DM6000 microscope. Images were analyzed using Matlab (MathWorks) software. Particle centers were tracked using custom-built software. To analyze nearest neighbor information, the Delaunay Triangulation function of Matlab was applied [36].

Magnetic fields were applied using a custom-built 5-pole electromagnet setup as shown in Figure 1b. Details and calibration data are given in the Supplementary Methods A.

Target capture experiments were performed with a model system consisting of protein G-coated M270 particles and fluorescently labeled antibodies as targets. The magnetic particles were coated with recombinant protein G (Thermo Scientific) following the specifications of the particle manufacturer. As targets, goat anti-mouse IgG labeled with Alexa fluor® 488 dye (Invitrogen) was used. Fluid chambers – blocked with BSA before the experiment – were filled with a 4 μL magnetic particle suspension (4×10^5 particles/μL) and, after 1 minute of settling time, followed by 34 μL of 110 pM target solution. The incubation process was studied without magnetic actuation and with magnetic actuation. In the latter case, a repeated sequence was applied of rotating fields for target capture (500 s) and interfacial rotaphoresis to redisperse particles over the surface (80 s). The actuation for target capture consists of a continuously rotating magnetic field (20 mT, 0.2 Hz) rotating in-plane with the surface (i.e., about the *z*-axis), combined with field gradients (4 T/m) oriented orthogonal to the bottom surface to move particles up and down through the fluid chamber. Particles were actively moved up and down through the fluid chamber to expose the particles to the whole fluid instead of only the fluid near the bottom surface of the fluid chamber. Target capture was quantified by recording fluorescence images using an EMCCD camera (Andor Luca S) after the incubation and by determining the fluorescence of the particles relative to the background using ImageJ software (http://rsbweb.nih.gov/ij/) and custom-written image analysis software in Matlab (Mathworks). More details are given in the Supplementary Methods E.

To simulate the particle behavior, we used a previously reported numerical model based on Brownian dynamics[35]. In short, the Brownian dynamics simulation of an N-particle system involves integrating the Langevin equation:

$$\frac{\partial}{\partial t} r_i = \sum_j^N \left(\mu_{ij} \cdot \nabla_{r_j} U(t) + \nabla \cdot D_{ij} \right) + v_i^{\mathrm{ran}}(t), \qquad (1)$$

where r_i is the position of particle i and μ_{ij} is the mobility matrix approximated by the Rotne-Prager-Blake tensor[11]. In particular, this tensor accounts for the hydrodynamic interactions of particles with other particles and with the surface. Furthermore, U(t) is the time-dependent interaction potential, that takes into account magnetic dipole-dipole interactions between all particles, field gradient forces, gravitational forces, and also excluded volume forces to account for steric repulsion between particles and the surface[35]. To include Brownian motion of the particles, a stochastic random velocity is introduced, which follows from the fluctuation-dissipation theorem[11,35]:

$$\left\langle \Delta r_i^{\mathrm{ran}}(t) \Delta r_j^{\mathrm{ran}}(t) \right\rangle = 2 k_{\mathrm{B}} T \mu_{ij} \delta t \,, \qquad (2)$$

in which Δr^{ran} is the random position vector, which relates to the random velocity. To compensate for the spatial variation in the particle mobility for Brownian motion, the term containing the diffusion tensor Dij = $k_{\mathrm{B}}T\mu_{ij}$ is used in Equation 1.[35] In the simulations, Equation 1 is solved with iterative time-steps of Δt = 2 μs which was found to be sufficiently small to generate consistent results[35].

3 Results

3.1 Interfacial rotaphoresis on small numbers of particles

In our system, the strong interfacial interaction originates from applied magnetic gradient forces that pull the particles to the surface, see Figure 1a. At the surface, hydrodynamic drag and hard-sphere collisions cause the particle assemblies to continuously change configuration over time. Figure 1c shows images of an experiment with superparamagnetic particles (∅ 2.8 μm, χ_p = 1.2, see Methods) which rapidly move and disperse over a surface. These dynamics are achieved by applying a magnetic field configuration with multiple elements to control the particle behavior, namely: (i) a field gradient pulls the particles towards the surface; (ii) the magnetic field aligns the particles in chains; (iii) a rotation of the field causes rotation and translation of the chains, while (iv) a small oscillating field component orthogonal to the rotating field creates a tilt to facilitate chain rotation (see Supplementary Information C and D). The direction of the velocity is given by the vectorial cross-product of the angular field velocity vector and the surface normal. Others have referred to the motion of individual rotating chains near a surface as 'artificial

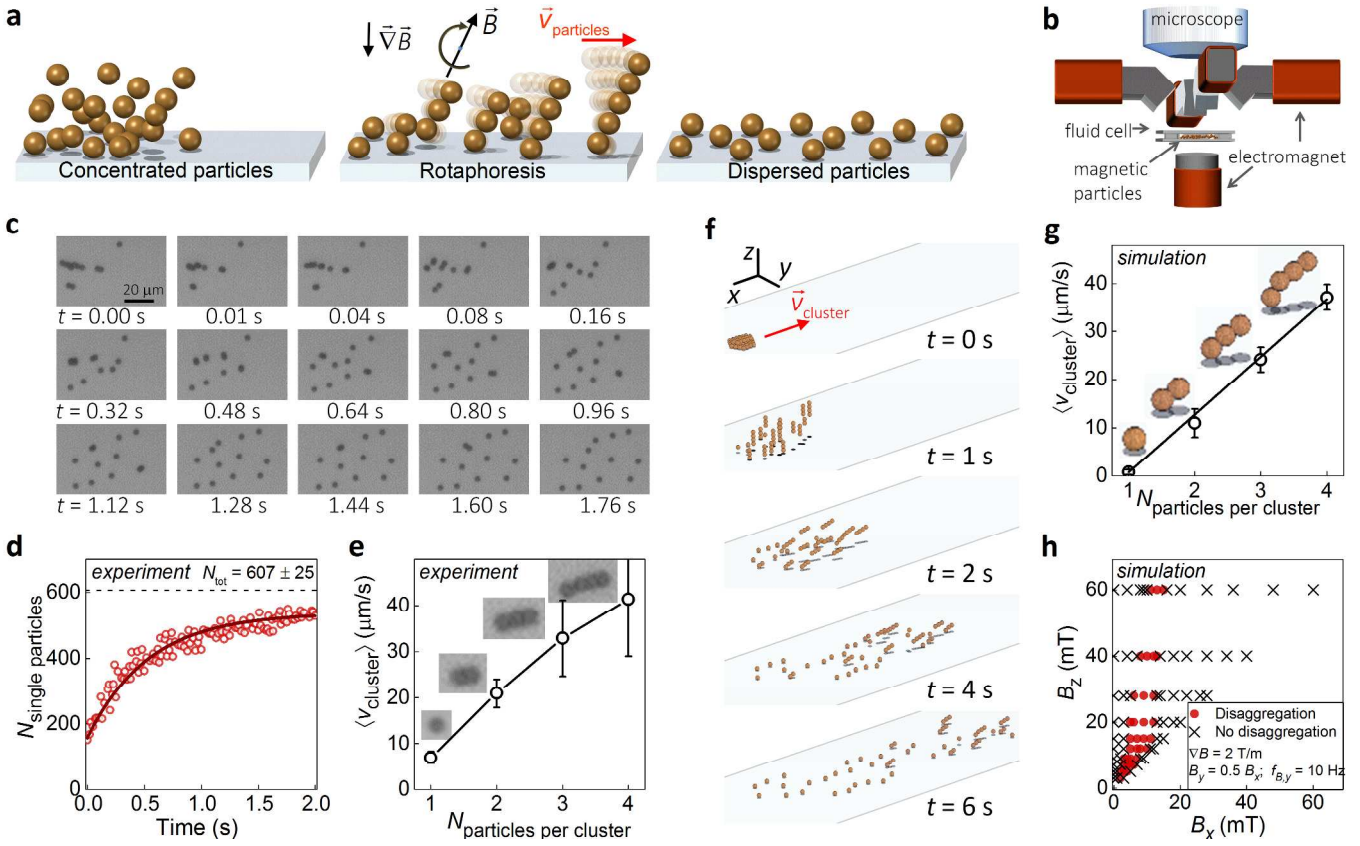

Figure 1. Principle of magnetic interfacial rotaphoresis and the microscale particle motion at the solid-liquid boundary. (a), Concept of magnetic interfacial rotaphoresis: A rotating field and a field gradient generate a dispersive motion along the surface. (b), 5-pole electromagnet used to manipulate the magnetic particles. (c), Microscope images showing the dispersion of a 12-particle (∅ 2.8 μm) assembly by interfacial rotaphoresis (left to right). (d), Time-dependence of the number of individual particles in an interfacial rotaphoresis experiment. The solid line corresponds to an exponential fit to the data. (e), Average rotaphoretic velocity of particle chains with different particle numbers, determined experimentally. Errors correspond to the standard deviation in the average velocity for different chains. (f), Snapshots of numerical simulations of a 40-particle (∅ 2.8 μm) cluster in a rotaphoretic field. (g), Average rotaphoretic velocity of particle chains with different particle numbers, determined in simulations. Error bars correspond to the standard deviation in the average velocity for different chains. The line corresponds to a least-squares linear fit to the data. (h), Influence of the relative size of the in-plane field component, Bx, and out-of-plane field component, Bz, of the rotating field on the disaggregation of a 40-particle cluster, determined by simulation.

swimming'[16], 'tumbling motion'[17] or 'colloidal walking'[11,28]. These terms are suited for dilute suspensions in which individual chains maintain chain integrity. In contrast, the chain configurations in our experiments are highly dynamic due to strong interaction with the surface (caused by the applied field gradient) and due to chain-chain interactions (caused by the high density of particles at the surface). Due to these conditions, our experiments show a broad range of phenomena, namely transportation, dispersion, as well as sub-monolayer ordering. Therefore we propose to use the term "magnetic interfacial rotaphoresis" to refer very generally to the principle of translational motion and spreading ('-phoresis') caused by magnetically-induced rotation at an interface.

From a microscopic study of the particle behavior, we find that interfacial rotaphoresis can disperse particle assemblies within several seconds (Figure 1c; Supplementary Video 1), showing a time constant of 0.6 s (Figure 1d). The induced displacement velocity scales almost linearly with the length of the particle assembly (Figure 1e). In simulations (see Methods) we used the same field configuration as in the experiments, and find the same rapid transportation and dispersive particle behavior (Figure 1f; Supplementary Video 2) and recovered a similar velocity scaling with the assembly size (Figure 1g). This proves that the colloid translation is caused by the hydrodynamic no-slip boundary condition and the hard-sphere collisions with the interface.

In addition, we characterized the range of in-plane (B_x) and out-of-plane (B_z) field components of the rotating field, for which particle alignment is completely suppressed. As shown in Figure 1h, clearly B_z needs to be larger than B_x. This can be understood from the fact that out-of-plane fields underly the repulsive interactions between the particles; the in-plane field components are needed to impose rotation on the chains, but also cause clusters to reform. For increased B_z, the allowed range of B_x does not increase linearly, which relates to the saturation of the particle magnetization[37], as the dipolar magnetic interaction depends on the particle magnetization and not directly on the external field.

3.2 Interfacial rotaphoresis on large numbers of particles

Interfacial rotaphoresis was studied on very large assemblies of magnetic particles, as shown in Figure 2. Starting with a massive and dense multilayer particle assembly with dimensions of about ~1 mm (~10^6 particles) positioned near one magnet pole, we applied interfacial rotaphoresis consecutively in four directions (north, east, south, west). The rotaphoretic actuation generates directional transport, redistribution, and dispersion of the particles over the surface, in the end leading to a hexagonal arrangement with a narrow distribution of particle-to-particle distances (see Figure 2a-c). Videos show that particles move over the surface in dispersing layers (see Supplementary Videos 3 and 4), with large clusters moving faster over the surface than small clusters, and non-clustered particles showing almost no translational motion (see Figure 1e,g). On a global scale, we observe that dense ensembles of particles displace faster than dilute ones (see Figure 2d-f), with velocities reaching several mm/s. The transportation and gradual dispersion of clusters causes the particles to evenly spread out over the surface (Figure 2a).

Clearly, interfacial rotaphoresis can control particle assemblies over a wide range of sizes and geometries: from massive, dense, millimeter-sized multilayer assemblies, down to assemblies consisting of just a few particles. By virtue of the effective translation and dispersion imposed on the particle assemblies, interfacial rotaphoresis is able to completely spread out colloidal assemblies, ending in a single-particle state where the dipolar alignment is frustrated for truly all particles; irrespective if the starting configuration consists of just a few particles, or if the starting configuration is large and dense.

3.3 Interfacial rotaphoresis to reversibly counter aggregation and drift

Magnetic particles are important in the field of lab-on-chip biosensing [13,21,26,27,38–41] as they allow the execution of key analytical process steps such as fluid mixing, analyte capture, buffer exchange, washing and detection. However, the handling of magnetic particles is fundamentally complicated by the tendency of the particles to magnetically aggregate and drift toward magnet poles. Figure 3a (see also Supplementary Video 5) shows how an applied rotation of particle chains about the *z*-

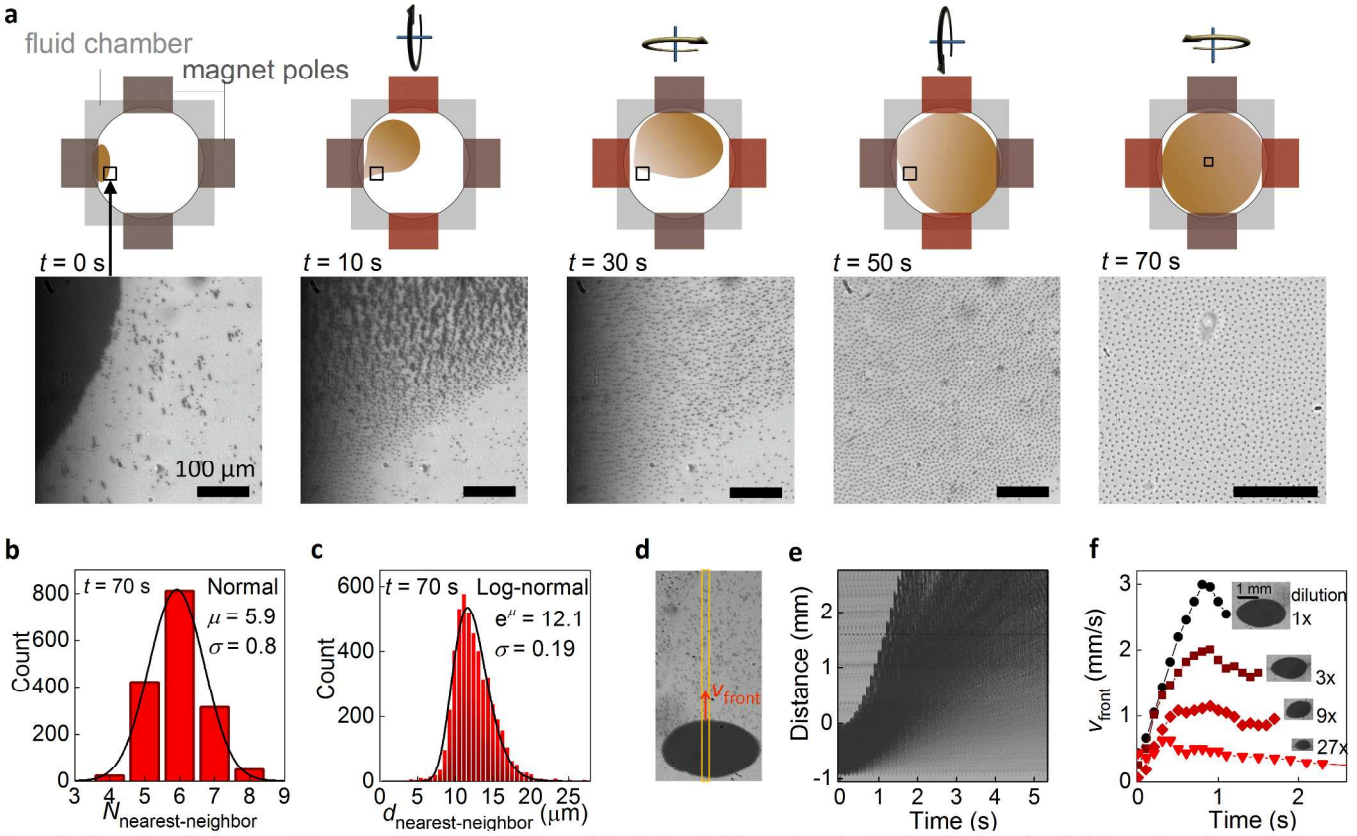

Figure 2. Dispersion of a large and dense ensemble of magnetic particles by interfacial rotaphoresis. (a), Sketch of the interfacial rotaphoresis experiment and corresponding series of microscopic topview images taken at selected locations in the fluid chamber. Starting at t = 0 with a large and dense cluster of particles at the west-side magnet pole, particles distribute over the surface by applying interfacial rotaphoresis consecutively in the north, east, south and west-ward direction. The image at t = 70 s demonstrates the final uniform particle distribution. The particles have a diameter of 2.8 µm. (b,c) Histograms of the number of nearest-neighbors per particle and of the nearest-neighbor distance, recorded in the dispersed particle state. (d), Microscope image of a concentrated pack of particles with a size of ~1.5 mm positioned at the center of the fluid chamber. The red arrow indicates the velocity of the particles at the front. The image is cropped from the sides according to the yellow rectangle to obtain (e), a kymograph of the response of the particles to a rotaphoretic field. (f), The velocity of the particles at the front of the pack during interfacial rotaphoresis, for different amounts of particles, as represented by the inset images with the same relative scales. Error bars (not shown) are 26 µm/s, corresponding to 2 pixels per image to determine the front position of the moving particle pack.

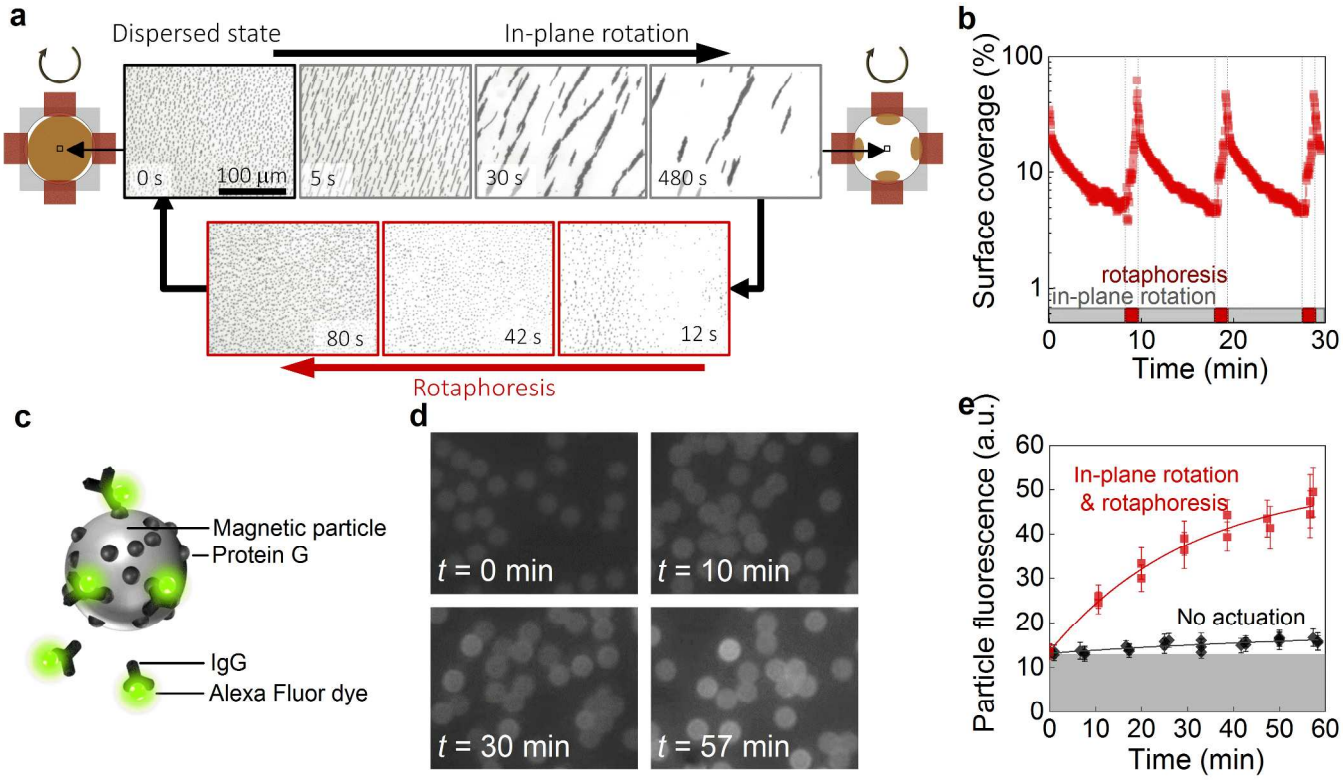

Figure 3. Interfacial rotaphoresis enables programmable particle assemblies for target capture in a microfluidic fluid volume. (a), A rotating magnetic field (6 mT, 0.1 Hz) about the *z*-axis causes particles (∅ 2.8 µm) to aggregate and drift away from the chamber center towards the magnet poles; the microscopy images are a top view of the center of the fluid chamber where the particle concentration decreases during the field rotation. The sketches on the left and the right side of the images show the location where the images are taken with respect to the fluid chamber and the magnet poles. Interfacial rotaphoresis recreates the original even particle distribution, which effectuates a system reset for further particle processing. (b), Coverage of the surface by particles as a function of time. The surface coverage is quantified using a threshold filter. The surface coverage is found to decrease when an rotating field is applied, caused by aggregate formation. Interfacial rotaphoresis recreates the original even particle distribution. (c), Model system to study the effect of interfacial rotaphoresis on target capture; fluorescently labeled antibodies were captured by protein G-coated magnetic particles. (d), Fluorescence images showing antibody capture as a function of time, for the system sketched in panel c. (e), Particle fluorescence measured as a function of time. The grey level marks the autofluorescence level of the particles (13.3 ± 0.4). The above-background fluorescence is caused by antibody capture onto the particles, studied for different protocols: no actuation (black diamonds), and rotation about the *z*-axis combined with interfacial rotaphoresis (red squares). Error bars correspond to the standard deviation in particle fluorescence. Solid lines correspond to fits of the form $I(t) = A(1-\exp(-k \cdot t)) + I_0$.

axis – applied to speed up microfluidic mixing and affinity capture[26,27] – generates clustering and thereafter drift of the particles away from the center toward the edges of the microfluidic chamber. Here, we show that the aggregation and drift can be counteracted by integrating pulses of interfacial rotaphoresis in an actuation scheme (see Figure 3a,b). Interfacial rotaphoresis is applied to rapidly disperse the particles over the surface; which we have demonstrated for particles with large and small sizes, with and without biological surface functionalizations, and in buffer as well as in complex fluids such as undiluted fetal bovine serum (see Supplementary Information B; Supplementary Video 6,7). Biofunctionalized particles often suffer from non-specific and adhesive interactions[42], especially when suspended in complex fluids. In the studied experimental conditions, interfacial rotaphoresis provides sufficient forces to overcome the inter-particle adhesion with a non-specific (bio)chemical origin.

Furthermore, we have integrated interfacial rotaphoresis in a biochemical incubation process. Magnetic stirring of particle chains in bulk fluid was alternated with interfacial rotaphoresis pulses to reset the particle distributions and counter drift and aggregation. We investigated the capture of analyte from solution by magnetic particles in a microfluidic cell (Fig 3c-e). A model system was used consisting of magnetic particles functionalized with protein G, which capture fluorescent IgG antibodies from the fluid. The captured antibody amount was detected via the fluorescence signal from the particles. As shown in Figure 3e, the actuation protocol that incorporated interfacial rotaphoresis increases the initial capture rate significantly, by 26 ± 7 times when compared to antibody capture without actuation. The assembly of ~10^5 particles very effectively samples the fluid volume without requiring any flow generation[43].

4 Discussion

4.1 Dependence of interfacial rotaphoresis on field and field gradient

Interfacial rotaphoresis of superparamagnetic colloids near a solid-liquid interface as shown in this paper, strongly depends on the configuration of the applied magnetic field. The main drivers for this process are the rotating magnetic field and the confining gradient force.

The rotating magnetic field is foremost characterized by the field strength and the rotation frequency. These parameters determine the ratio of (respectively) the magnetic and hydrodynamic torques which act on the particle chains[34], and thereby govern the general rotational behavior of a particle chain. In case a particle chain is suspended in an unbounded fluid (i.e. without solid-liquid interface), an increased field frequency (or decreased field strength) leads to periodic fragmentation of the particle chain into smaller particle chains. In the presence of a solid-liquid interface, rotating chains encounter additional forces which hamper the rotation, leading to further fragmentation, or, if the magnetic dipolar forces between the particles are strong enough, leading to translation as the rotation axis shifts towards the contact point with the surface (see also Supplementary information D).

It is insightful to qualitatively describe how the translational motion of the magnetic particles relates to the frequency of the rotating field, i.e. at constant and nonzero field strength and magnetic field gradient. In the limit of a zero field rotation frequency, large chains of particles are formed and no translation is induced. For low field rotation frequencies, chains relatively slowly erect themselves from the surface and thereby translate. In this case the particle chains remain large and single rotations lead to large steps, but the step frequency is low. Increasing the field rotation frequency at first does not fragment the particle chains but does increase the step frequency, and thereby leads to an increased translation velocity. Increasing the field rotation frequency even further, chains start to fragment into smaller chains and this leads to a reduced step size per rotation. At a certain frequency a maximum translation velocity is reached, where the product of step length and step frequency is optimal. For frequencies beyond the optimum, the reduction of chain length and step size becomes more important than the increase of step frequency. At very high rotation frequencies the translation velocity approaches zero. Similarly, a maximum of translation velocity is observed when varying the field magnitude at constant rotation frequency, because the rotation behavior of a particle chain depends on the ratio between the field rotation frequency and the magnetic field strength (see also Supplementary information D)[34].

The magnetic field gradient that is oriented toward the surface has the following effect on the particle translation velocity. For small magnetic field gradients, the translation velocity is low, as a rotating chain erects and thereby moves away from the surface. It therefore only very weakly and briefly interacts with the surface, namely only when oriented perpendicular to the surface. With an increase of the strength of the field gradient, the chain is pulled toward the surface, thereby the contact time is increased, and with it the translation velocity. However, when the field gradient becomes very high, the particle chain is not anymore able to complete a full rotation, because it is strongly pulled onto the surface and cannot be erected by the rotating field. So for very strong field gradients, a zero translation velocity is observed. So also for the magnetic field gradient, a magnitude exists where the translation velocity is maximal.

The main function of the magnetic field gradient is to confine the magnetic colloids at the solid-liquid interface. The typical confinement distance is determined by the thermal energy divided by the magnetic force. The magnetic gradient force scales with the applied magnetic field gradient and the particle magnetic moment. Small particles typically have smaller magnetic moments than large particles, therefore higher field gradients are needed to confine small particles at a surface. In our experiments particles were used with diameters in the range between 2.8 μm and 0.5 μm. For these particles, all interfacial rotaphoresis phenomena have been observed, namely transportation, complete dispersion, and sub-monolayer ordering. For smaller particles, we expect that magnetic fields, field gradients and/or particle magnetizations must be increased for all assembly phenomena to be observable.

4.2 Comparison of interfacial rotaphoresis-assisted dispersion with other techniques

Here we compare interfacial rotaphoresis-assisted dispersion to other dispersion methods that have been reported in the literature for colloid-based lab-on-chip applications. To redistribute particles, particle clusters need to break up and disaggregate into separate particles. A method that is commonly applied to superparamagnetic particles, is to simply remove the magnetic field (e.g. see[13,44]) in order to allow Brownian motion to separate the clustered particles. However, thermal forces are small and therefore the disaggregation is a slow process with limited effectiveness. More often than not particles remain largely clustered. This is particularly the case in practical applications where the particle surfaces are modified, for example, when particles are functionalized with reactive molecules (e.g. proteins) and/or suspended in buffer solutions (with salts that efficiently shield the surface charges) or in complex matrices such as undiluted plasma (clear data on this topic was shown by Ranzoni et al.[13]).

To overcome adhesive interactions between particles, the particle functionalization can be changed[13] and active forces can be applied. In previous work[35,45], we have studied particle disaggregation near a solid-liquid boundary by a field-switch method, i.e. by switching the field by 90 degrees, between an out-of-plane and in-plane orientation with respect to the surface. For symmetry reasons, a 90 degrees switching method cannot generate a net translation of particles over the surface. Furthermore, the method cannot completely suppress the occurrance of multi-particle alignment, and the method is only applicable in the limit of very dilute particle suspensions and

small cluster sizes ($N < 10^2$), not for high particle densities and cluster sizes as used in most applications ($N > 10^5$). Magnetic interfacial rotaphoresis is a fundamentally different way to actuate magnetic particles. Magnetic interfacial rotaphoresis gives highly effective translation, dispersion as well as disaggregation of particle clusters (down to single-particle level) for realistic particle densities and cluster sizes ($N > 10^5$) within a timescale of a few seconds.

An alternative method to disperse magnetic particles within a fluid volume is the application of ultrasound[46]. Using ultrasound, clustered particles can be effectively disaggregated and mixed with the fluid. A first inherent difference is that ultrasound couples to the fluid as well as to the particles, while magnetic fields couple only to the particles. A second difference is that ultrasound lacks the strong short-range dipolar forces present in magnetic actuation. This makes magnetic actuation particularly suited for ordering effects, for application to small colloidal particles, and for the control of particle assemblies near a surfac

4.3 Interfacial rotaphoresis and other rotation-translation concepts

Here we compare interfacial rotaphoresis with other rotation-translation concepts. In a theoretical paper, Bonthuis et al.[47] studied the application of rotating electric fields to an electroneutral dipolar fluid (pure water) in nanochannels. The applied electric field rotates the water molecules and the injected torque is converted into flow vorticity, and thereby the rotating field generates a net fluid flow. The underlying physics is very different from our system, because electric fields are used rather than magnetic fields and because the torque is imposed on molecules rather than on particles. Furthermore, the concept of Bonthuis et al. is focused on the generation of convective flow rather than dispersion, and it is not suited for biological fluids because dissolved salts strongly perturb electrical effects.

The translational motion of isolated particle chains rotating near a surface has been studied by several groups[11,16,17] In these studies the particle concentrations were kept low and interactions between rotating chains were avoided. In contrast, interfacial rotaphoresis as described in this paper has been designed to effectuate a highly effective translation and dispersion of particles over a surface for a very wide range of particle densities. The applied field gradient force creates a strong interaction of the particles with the surface, giving velocities of mm/s. The high velocity in combination with a high particle density gives a very high net flux of colloidal particles over the surface.

Concerning the particle transportation functionality, it is interesting to compare on the one hand transportation due to *interfacial rotaphoresis* as described in this paper, and on the other hand transportation due to *bulk flow* generated by a collective rotational motion of magnetic particle chains in a fluid cell[11]. In the bulk flow concept, particles bring fluid into motion, which in turn transports the particles. This is an indirect transportation principle. The concept uses large particles (10 μm) with a mass density that is similar to water (1.1×10^3 $kg.m^{-3}$). Additionally, the global fluid flow is dependent on the geometry of the fluid chamber containing the particle suspension. Magnetic interfacial rotaphoresis is an interface phenomenon that directly imposes a translational motion on the particles, independent of the shape of the fluid chamber. Magnetic interfacial rotaphoresis is insensitive to the particle mass density and works well for a wide range of particle types and particle sizes (500 nm – 2.8 μm in our experiments). In addition to the transportation functionality, interfacial rotaphoresis is able to completely disperse even dense colloidal assemblies, and is able to repeatedly arrange the particles into an ordered submonolayer structure, which is not possible with a bulk flow concept.

5. Conclusions

We have revealed magnetic interfacial rotaphoresis as a principle to manipulate dense assemblies of magnetic colloids near a solid-liquid interface, reporting a versatile set of functionalities (translation, dispersion, as well as ordering) caused by rotating fields and strong interaction with a solid boundary, in a parameter space where magnetic, hydrodynamic and solid-liquid boundary interactions are balanced. Interfacial rotaphoresis transforms dense and large particle assemblies into single particles, based on dispersive size-dependent translational velocities of several millimeters per second. The observed multi-functionality is operational for a wide range of biochemical conditions and colloid sizes (500 nm – 2.8 μm in our experiments). The ability to reversibly manipulate high densities and high numbers of colloids ($N > 10^5$) by interfacial rotaphoresis was demonstrated in a colloid-based molecular capture experiment.

We expect that this work will lead to further discoveries of colloidal assembly phenomena in dynamic magnetic fields. The dispersive forces may be expected to support particle ordering and separation effects e.g. based on size, shape, and magnetic properties. Furthermore, it will be interesting to study the dependence of transportation, dispersion and ordering phenomena on macromolecular fluid composition and colloidal surface functionalizations, as these represent handles to modulate inter-particle and particle-surface interactions. Finally, capillary interactions may be introduced in the system by studying the particle assembly processes at liquid-liquid interfaces, where surface tension forces will strongly influence the dynamics of the particles. We foresee that further studies will reveal more unexpected colloid assembly phenomena and will open new avenues to fabricate and dynamically operate colloid-based devices.

Acknowledgements

We thank Peter Zijlstra, Tom de Greef, Wouter Ellenbroek, Henk Swagten, and Herman Clercx for their valuable comments. Part of this work was funded by the Dutch

Technology Foundation (STW) under grant number 10458.

Notes and references

[a] Department of Applied Physics, Eindhoven University of Technology, 5600 MB Eindhoven, The Netherlands
Institute for Complex Molecular Systems, Eindhoven University of Technology, 5600 MB Eindhoven, The Netherlands
[b] Department of Biomedical Engineering, Eindhoven University of Technology, 5600 MB Eindhoven, The Netherlands
Email: m.w.j.prins@tue.nl

Electronic Supplementary Information (ESI) available: A. Interfacial rotaphoresis experiments. B. Interfacial rotaphoresis for different types of particles C. Particle behavior for different rotaphoretic field configurations. D. Estimation of the ratio of torques in interfacial rotaphoresis. E. Experiments on particle-based capture of antibodies from a fluid. F. Supplementary Videos. See DOI: 10.1039/b000000x/

1 Y. A. Vlasov, X. Z. Bo, J. C. Sturm and D. J. Norris, *Nature*, 2001, **414**, 289–293.
2 J. C. Loudet, P. Barois and P. Poulin, *Nature*, 2000, **407**, 611–613.
3 A. I. Hochbaum, R. Fan, R. He and P. Yang, *Nano Lett*, 2005, **5**, 457–460.
4 A. N. Shipway, E. Katz and I. Willner, *Chemphyschem*, 2000, **1**, 18–52.
5 R. Elghanian, J. J. Storhoff, R. C. Mucic, R. L. Letsinger and C. A. Mirkin, *Science (80-.).*, 1997, **277**, 1078–1081.
6 Y. Li, W. Cai and G. Duan, *Chem. Mater.*, 2008, **20**, 615–624.
7 F. Li, D. P. Josephson and A. Stein, *Angew Chem Int Ed Engl*, 2011, **50**, 360–388.
8 J. E. Martin and A. Snezhko, *Rep Prog Phys*, 2013, **76**, 126601.
9 R. M. Erb, H. S. Son, B. Samanta, V. M. Rotello and B. B. Yellen, *Nature*, 2009, **457**, 999–1002.
10 Y. Wang, Y. Gao, H. Wyss, P. Anderson and J. den Toonder, *Lab Chip*, 2013, **13**, 3360–3366.
11 C. E. Sing, L. Schmid, M. F. Schneider, T. Franke and A. Alexander-Katz, *Proc Natl Acad Sci U S A*, 2010, **107**, 535–540.
12 Y. Gao, J. Beerens, A. van Reenen, M. A. Hulsen, A. M. de Jong, M. W. J. Prins and J. M. J. den Toonder, *Lab Chip*, 2015, **15**, 351–60.
13 A. Ranzoni, G. Sabatte, L. J. van IJzendoorn and M. W. J. Prins, *ACS Nano*, 2012, **6**, 3134–3141.
14 L. J. Hill and J. Pyun, *ACS Appl Mater Interfaces*, 2014, **6**, 6022–6032.
15 L. He, M. Wang, J. Ge and Y. Yin, *Acc Chem Res*, 2012, **45**, 1431–1440.
16 P. Tierno, R. Golestanian, I. Pagonabarraga and F. Sagués, *Phys. Rev. Lett.*, 2008, **101**, 218304.
17 H. Morimoto, T. Ukai, Y. Nagaoka, N. Grobert and T. Maekawa, *Phys. Rev. E*, 2008, **78**, 021403.
18 Y. Yang, L. Gao, G. P. Lopez and B. B. Yellen, *ACS Nano*, 2013, **7**, 2705–2716.
19 A. F. Demirors, P. P. Pillai, B. Kowalczyk and B. A. Grzybowski, *Nature*, 2013, **503**, 99–103.
20 N. Osterman, I. Poberaj, J. Dobnikar, D. Frenkel, P. Ziherl and D. Babic, *Phys. Rev. Lett.*, 2009, **103**, 228301.
21 D. M. Bruls, T. H. Evers, J. A. H. Kahlman, P. J. W. van Lankvelt, M. Ovsyanko, E. G. M. Pelssers, J. J. H. B. Schleipen, F. K. de Theije, C. A. Verschuren, T. van der Wijk, J. B. A. van Zon, W. U. Dittmer, A. H. J. Immink, J. H. Nieuwenhuis and M. W. J. Prins, *Lab Chip*, 2009, **9**, 3504–3510.
22 M. Herrmann, E. Roy, T. Veres and M. Tabrizian, *Lab Chip*, 2007, **7**, 1546–1552.
23 D. Du, D. Li, M. Thakur and S. L. Biswal, *Soft Matter*, 2013, **9**, 6867.
24 J. Yan, S. C. Bae and S. Granick, *Soft Matter*, 2015, **11**, 147–53.
25 K. J. Solis and J. E. Martin, *Soft Matter*, 2014, **10**, 6139.
26 A. van Reenen, A. M. de Jong, J. M. J. den Toonder and M. W. J. Prins, *Lab Chip*, 2014, **14**, 1966–86.
27 M. A. Gijs, F. Lacharme and U. Lehmann, *Chem Rev*, 2010, **110**, 1518–1563.
28 J. P. Steimel, J. L. Aragones and A. Alexander-Katz, *Phys. Rev. Lett.*, 2014, **113**, 178101.
29 K. C. Neuman and A. Nagy, *Nat Methods*, 2008, **5**, 491–505.
30 E. K. Sackmann, A. L. Fulton and D. J. Beebe, *Nature*, 2014, **507**, 181–189.
31 B. A. Grzybowski, H. A. Stone and G. M. Whitesides, *Nature*, 2000, **405**, 1033–1036.
32 G. Kokot, D. Piet, G. M. Whitesides, I. S. Aranson and A. Snezhko, *Sci. Rep.*, 2015, **5**, 9528.
33 M. Belkin, a. Snezhko, I. S. Aranson and W. K. Kwok, *Phys. Rev. Lett.*, 2007, **99**, 1–4.
34 Y. Gao, M. A. Hulsen, T. G. Kang and J. M. J. den Toonder, *Phys. Rev. E*, 2012, **86**, 41503.
35 A. van Reenen, Y. Gao, M. A. Hulsen, A. M. de Jong, J. M. J. den Toonder and M. W. J. Prins, *Phys Rev E Stat Nonlin Soft Matter Phys*, 2014, **89**, 042306.
36 D. Lee and B. Schachter, *Int. J. Comput. Inf. …*, 1980, **9**, 219–242.
37 A. Van Reenen, Y. Gao, A. H. Bos, A. M. De Jong, M. A. Hulsen, J. M. J. Den Toonder and M. W. J. Prins, *Appl. Phys. Lett.*, 2013, **103**, 043704.
38 R. Gottheil, N. Baur, H. Becker, G. Link, D. Maier, N. Schneiderhan-Marra and M. Stelzle, *Biomed Microdevices*, 2014, **16**, 163–72.
39 R. S. Gaster, D. A. Hall, C. H. Nielsen, S. J. Osterfeld, H. Yu, K. E. Mach, R. J. Wilson, B. Murmann, J. C. Liao, S. S. Gambhir and S. X. Wang, *Nat Med*, 2009, **15**, 1327–1332.
40 R. C. den Dulk, K. A. Schmidt, G. Sabatte, S. Liebana and M. W. J. Prins, *Lab Chip*, 2013, **13**, 106–118.
41 J.-M. Nam, C. S. Thaxton and C. A. Mirkin, *Science*, 2003, **301**, 1884–6.
42 K. J. M. Bishop, C. E. Wilmer, S. Soh and B. a Grzybowski, *Small*, 2009, **5**, 1600–30.
43 T. M. Squires, R. J. Messinger and S. R. Manalis, *Nat. Biotechnol.*, 2008, **26**, 417–426.
44 G. Degre, E. Brunet, A. Dodge and P. Tabeling, *Lab Chip*, 2005, **5**, 691–694.
45 Y. Gao, A. van Reenen, M. a Hulsen, A. M. de Jong, M. W. J. Prins and J. M. J. den Toonder, *Lab Chip*, 2013, **13**, 1394–401.
46 M. Wiklund, S. Radel and J. J. Hawkes, *Lab Chip*, 2013, **13**, 25–39.
47 D. Bonthuis, D. Horinek, L. Bocquet and R. Netz, *Phys. Rev. Lett.*, 2009, **103**, 144503.

Graphical abstract